Computer Assisted Mechanics and Engineering Sciences, 7: 81–90, 2000.

Computation of stress intensity factors by the compliance approach

Sameer A. Hamoush
Department of Architectural Engineering, North Carolina A&T State University, Greensboro, NC 27411 USA

Hisham Abdel-Fattah
Department of Civil Engineering, Kuwait University, Kuwait

(Received March 24, 1999)

A numerical method based on compliance approach is presented for analyzing an isotropic homogeneous sheet enclosing a crack. The method calculates the strain energy release rate and determines the stress intensity factors K_{I} and K_{II}. This method is suitable for any load combination in pure mode I, pure mode II and mix mode loading. A simple and efficient solution approach is developed in which the strain energy release rate is calculated by combining the finite element method with the fundamental relationships in fracture mechanics. The solution technique converges to accurate results for a small crack extension of the finite element mesh. The solution approach is also shown to be suited for separating the mode I and mode II stress intensity factors for a mixed mode loading. Numerical examples are presented to demonstrate the accuracy of the proposed approach.

Keywords: strain energy release rate, stress intensity factors, finite element analysis, mixed mode loading, compliance approach

1. Introduction

The computation of the stress intensity factors of cracks has received considerable attention in the literature. Analytical methods were developed in closed form solutions for special cases with specific loading configuration [7]. However, these solutions are for specific geometry and loading. For more general configuration of loading and geometry, numerical approach is necessary to evaluate the stress intensity factors.

In conjunction with the finite element method, the J-integral approach was used by several researchers [1, 3, 5] to evaluate the stress intensity factors. Other techniques such as the crack closure integral [2] and the stiffness derivative [4] were implemented for the same purpose.

In this paper, an alternate method based on the compliance technique is developed to calculate the total energy release rate. The numerical examples presented demonstrate the accuracy of the proposed approach in calculating the pure mode I and mode II stress intensity factors as well as the separation of the two modes in a mixed mode loading.

2. Formulation

When a crack in an isotropic homogeneous media of length a extends to a new length $a + \Delta a$, the strain energy release rate G is defined as shown in [6].

$$G = \lim_{\Delta A \to 0} \frac{\Delta U}{\Delta A} \tag{1}$$

where ΔU is the change in the potential energy and ΔA the formed new crack area when the crack extension takes place.

The strain energy release rate for plane stress conditions can be expressed in terms of the stress intensity factors as follows,

$$G = \frac{K_{\mathrm{I}}^2 + K_{\mathrm{II}}^2}{E} \,. \tag{2}$$

Equation (2) relates the strain energy release rate G to the stress intensity factors for mode I (K_{I}) and mode II (K_{II}). For a single mode problem, the stress intensity factor can be evaluated directly by Eq. (2) based on the knowledge of the strain energy release rate.

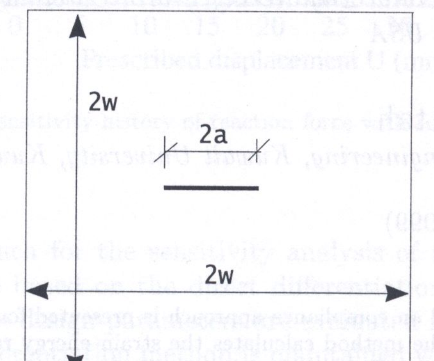

Fig. 1. The analyzed plate with center crack

If the crack shown in Fig. 1 extends by a very small increment Δa from a length $2a$ to a new length of $2a + 2\Delta a$ under the applied external loads f_i; the strain energy release rate can be expressed numerically as follows:

$$G = \frac{1}{8\Delta ab} \sum (f_i)\Delta v_i \tag{3}$$

where, Δv_i are the change in load displacements in direction of the load f_i when the crack extends from the length $2a$ to the new length $2a + 2\Delta a$, b is the thickness of the specimen.

The strain energy release rate calculated by Eq. (3) depends on the amount of the crack extension Δa. To show the convergence of Eq. (3), numerical investigation is performed in the following section.

3. Numerical investigation

The technique described in the preceding section has been incorporated into a conventional finite element code. Four node elements are used in the finite element mesh shown in Fig. 2. The finite element mesh is optimized based on the study performed in [2, 3, 4]. It was noted that the finite element solution converges when a total of 424 elements and 482 nodes are used in the analysis. All elements of the mesh have an aspect ratio below 5. The discretization of the mesh is done in a manner such that the number of elements and nodes is kept constant when a change in crack extension is processed. This implies changing the elements discretization of the continuum in the crack tip zone as shown in Fig. 2.

3.1. Pure mode I and pure mode II stress intensity factors

The computation of stress intensity factors for pure mode I loading and pure mode II loading of the plate shown in Fig. 1 is analyzed. An isotropic homogeneous plate enclosing a center crack with the ratio $2w/2a$ of 10 is studied.

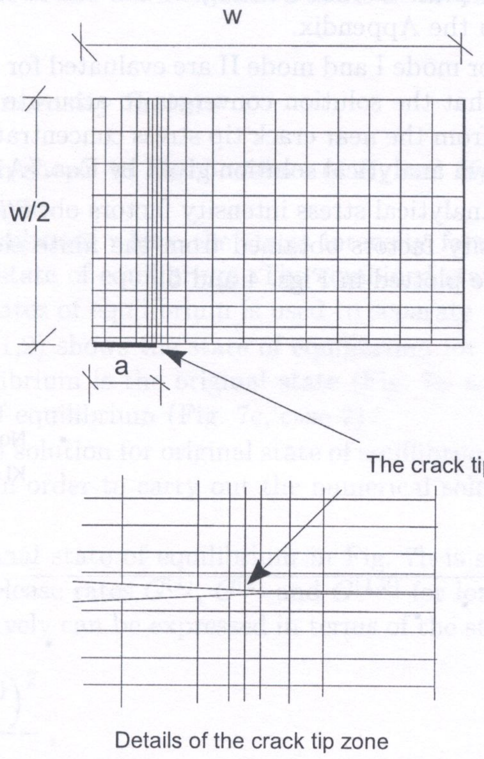

Fig. 2. One fourth of the finite element mesh

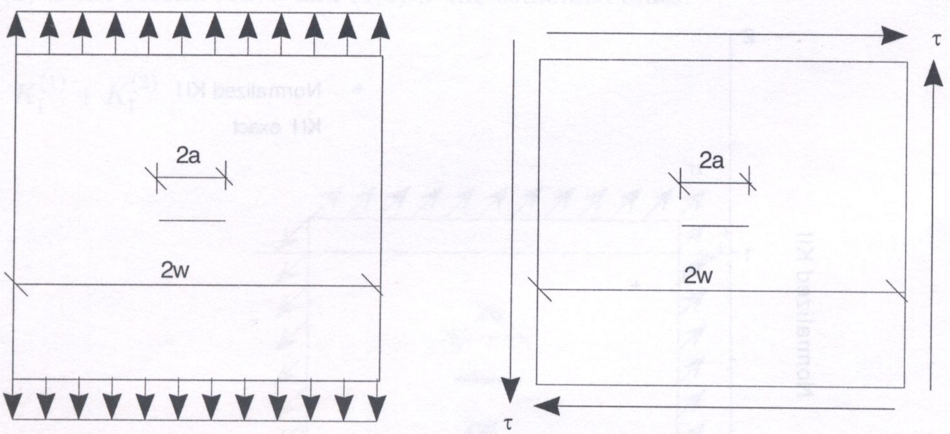

Fig. 3. The analyzed plate in pure mode I and pure mode II

For the pure mode I modeling, a normal tensile stress equal to 100 MPa is applied at the edges as shown in Fig. 3. For the pure mode II modeling, a uniform shear stress equal to 100 MPa is applied at the boundaries of the plate as shown in Fig. 3. The closed form asymptotic solutions for the above problems are given in the Appendix.

The stress intensity factors for mode I and mode II are evaluated for crack extensions in the range of $[0.005a\text{–}0.5a]$. It was noted that the solution converges to accurate values for a crack extension close to the crack tip and away from the near crack tip stress concentration. The obtained numerical results are compared to the known analytical solution given by Eqs. (A1) and (A2) in the Appendix.

The difference between the analytical stress intensity factors obtained from Eqs. (A1) and (A2), and the numerical stress intensity factors obtained from the finite element solutions for different values of crack extension Δa are plotted in Figs. 4 and 5.

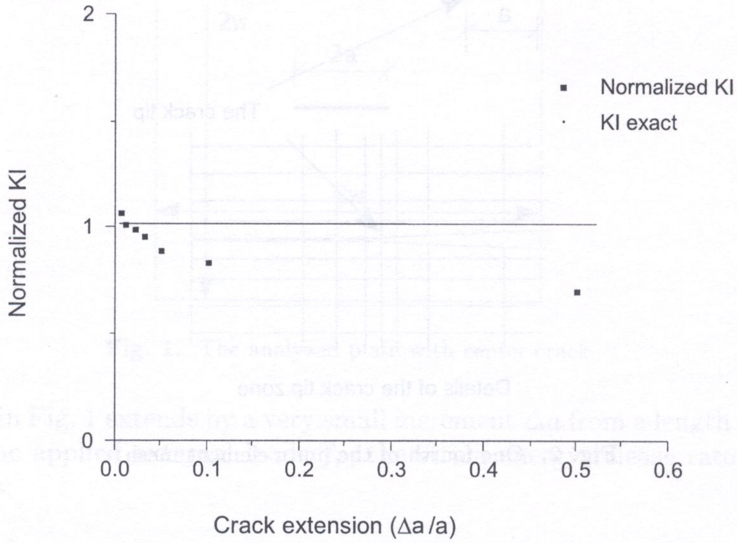

Fig. 4. The normalized stress intensity factor for mode I in a pure opening mode problem versus the crack extension Δa

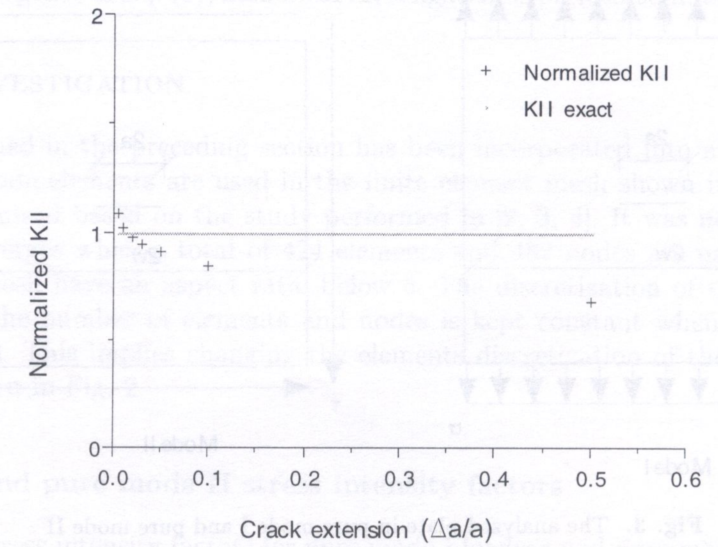

Fig. 5. The normalized stress intensity factor for mode II in a pure sliding mode problem versus the crack extension Δa

Figure 4 shows the variation of the normalized K_{I} with crack extension Δa and Fig. 5 shows the variation of the normalized K_{II}. The results show that values of the stress intensity factors become more accurate when the value of the crack extension Δa is in the neighboring of the value of $0.01a$.

3.2. Mixed mode stress intensity factors

For the mixed mode problem shown in Fig. 6, values of K_{I} and K_{II} can be separated by superimposing two states of equilibrium.

The original state of equilibrium where the stress intensity factors need to be evaluated is superimposed by an auxiliary state of equilibrium. The combined state of equilibrium in conjunction with the two independent states of equilibrium is used to separate the stress intensity factors.

Figure 7a (noted as case 1,2) shows the state of equilibrium for two combined states of equilibrium, the first state of equilibrium is the original state (Fig. 7b noted as case 1), and the second state is the auxiliary state of equilibrium (Fig. 7c, case 2).

The analytical closed form solution for original state of equilibrium (Fig. 7b) is given by Eqs. (A3) and (A4) in the Appendix. In order to carry out the numerical solution, the formulation is carried out as follows:

To evaluate K_{I}, the original state of equilibrium in Fig. 7b is super imposed over the state in Fig. 7c. The strain energy release rates $G^{(1)}$, $G^{(2)}$ and $G^{(1,2)}$ for loading in states (1), (2), and the combined state (1,2) respectively can be expressed in terms of the stress intensity factors as follows:

$$G^{(1)} = \frac{\left(K_{\mathrm{I}}^{(1)}\right)^2 + \left(K_{\mathrm{II}}^{(1)}\right)^2}{E}, \tag{4}$$

$$G^{(2)} = \frac{\left(K_{\mathrm{I}}^{(2)}\right)^2}{E}, \tag{5}$$

$$G^{(1,2)} = \frac{\left(K_{\mathrm{I}}^{(1,2)}\right)^2 + \left(K_{\mathrm{II}}^{(1,2)}\right)^2}{E}. \tag{6}$$

The numeric superscripts in Eqs. (4)–(6) indicate the specific state of equilibrium where (1) is the first state, (2) is the second state, and (1,2) is the combined state.

Since

$$K_{\mathrm{I}}^{(1,2)} = K_{\mathrm{I}}^{(1)} + K_{\mathrm{I}}^{(2)}$$

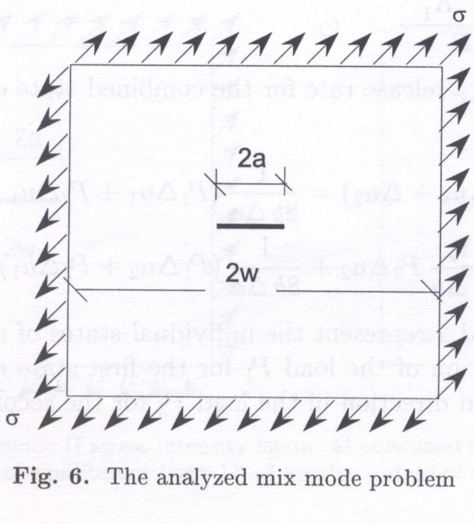

Fig. 6. The analyzed mix mode problem

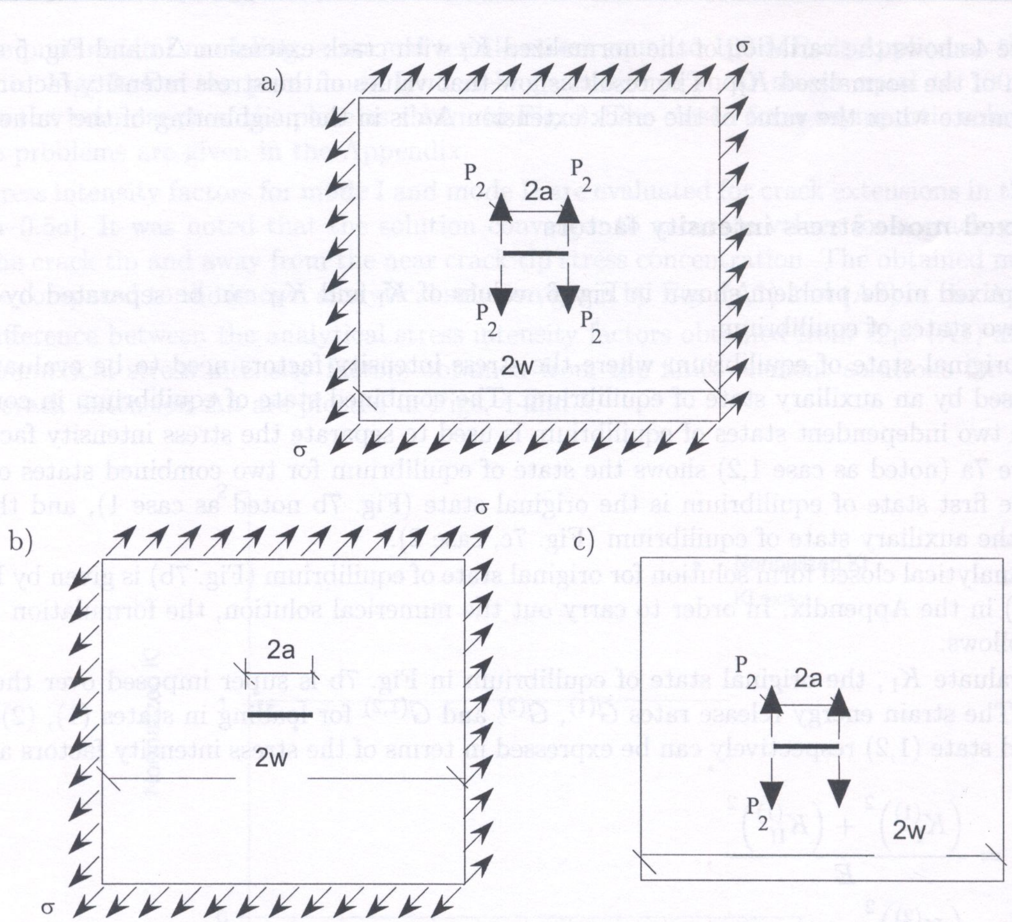

Fig. 7. Separation of the mode I stress intensity factor: a) combined state of equilibrium (case 1,2); b) original state of equilibrium (case 1); c) auxiliary state of equilibrium (case 2)

and

$$K_{\mathrm{II}}^{(1,2)} = K_{\mathrm{II}}^{(1)},$$

therefore, Eqs. (4), (5) and (6) can be combined as follows,

$$G^{(1,2)} = \frac{\left(K_{\mathrm{I}}^{(1)} + K_{\mathrm{I}}^{(2)}\right)^2 + \left(K_{\mathrm{II}}^{(1)}\right)^2}{E} = \frac{\left(K_{\mathrm{I}}^{(1)}\right)^2}{E} + \frac{\left(K_{\mathrm{II}}^{(1)}\right)^2}{E} + \frac{\left(K_{\mathrm{I}}^{(2)}\right)^2}{E} + \frac{2K_{\mathrm{I}}^{(1)}K_{\mathrm{I}}^{(2)}}{E}$$

$$= G^{(1)} + G^{(2)} + \frac{2K_{\mathrm{I}}^{(1)}K_{\mathrm{I}}^{(2)}}{E}. \tag{7}$$

But the numerical strain energy release rate for the combined state of equilibrium for a thickness b is given by

$$G^{(1,2)} = \frac{1}{8b\,\Delta a}(P_1 + P_2)(\Delta u_1 + \Delta u_2) = \frac{1}{8b\,\Delta a}(P_1\Delta u_1 + P_2\Delta u_1 + P_1\Delta u_2 + P_2\Delta u_2)$$

$$= \frac{1}{8b\,\Delta a}P_1\Delta u_1 + \frac{1}{8b\,\Delta a}P_2\Delta u_2 + \frac{1}{8b\,\Delta a}(P_1\Delta u_2 + P_2\Delta u_1). \tag{8}$$

In Eq. (8), the subscripts 1 and 2 represent the individual states of equilibrium. Δu_1 is the change in load displacements in direction of the load P_1 for the first state of equilibrium, and Δu_2 is the change in load displacements in direction of the load P_2 for the second state of equilibrium. Since

$$G^{(1)} = \frac{1}{8b\,\Delta a}P_1\Delta u_1 \tag{9}$$

and

$$G^{(2)} = \frac{1}{8b\,\Delta a}\,P_2\Delta u_2\,, \tag{10}$$

therefore, Eq. (8) becomes

$$G^{(1,2)} = G^{(1)} + G^{(2)} + \frac{1}{8b\,\Delta a}\,(P_1\Delta u_2 + P_2\Delta u_1)\,. \tag{11}$$

When b equals to one unit, Eqs. (7) and (11) lead to:

$$\frac{1}{8\Delta a}\,(P_1\Delta u_2 + P_2\Delta u_1) = \frac{2K_{\rm I}^{(1)}\,K_{\rm I}^{(2)}}{E}\,. \tag{12}$$

Equation (12) is used to determine the mode I stress intensity factor $K_{\rm I}^{(1)}$. In order to determine values of P_2 and Δu_2, the known closed form solution of the auxiliary state of equilibrium is used in which $K_{\rm I}^{(2)}$ is assigned to be equal to 1. The value of P_2 is calculated using Eq. (A5) given in the Appendix.

The values of Δu_1 and Δu_2 are obtained numerically using the finite element program. Thus, for each crack extension Δa, the value of $K_{\rm I}^{(1)}$ can be calculated.

A similar method is used to separate the mode II stress intensity factor. The state shown in Fig. 8a is the superposition of two states of equilibrium (noted as case (1,2)). Fig. 8b is the original

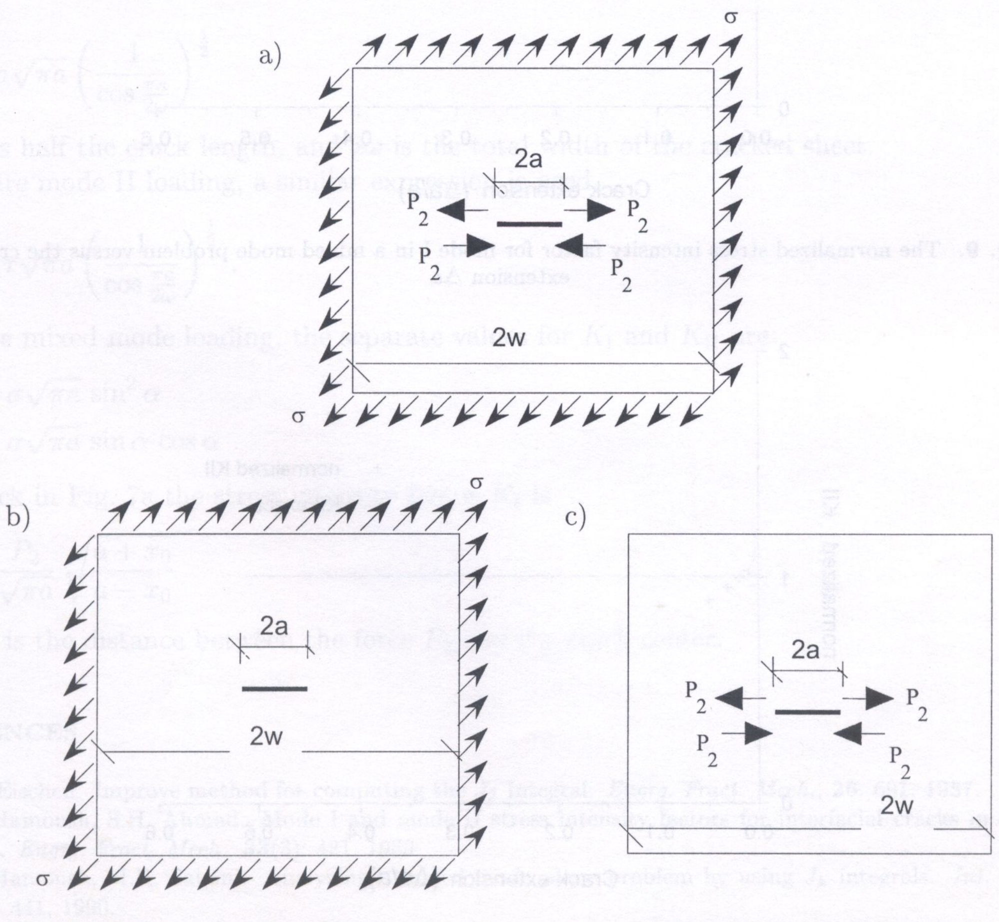

Fig. 8. Separation of the mode II stress intensity factor: a) combined state of equilibrium (case 1,2); b) original state of equilibrium (case 1); c) auxiliary state of equilibrium (case 2)

state and Fig. 8c is the auxiliary state. The $K_{II}^{(1)}$ is calculated in the same manner as $K_I^{(1)}$. The final equation is given as

$$\frac{1}{8\Delta a}\left(P_1\Delta u_2 + P_2\Delta u_2\right) = \frac{2K_{II}^{(1)}K_{II}^{(2)}}{E}\,.$$

The normalized plots of K_I and K_{II} versus the crack extension Δa. are shown in Figs. 9 and 10. It can be noticed that the numerical scheme's convergence is directly related to the magnitude of crack extension Δa. The calculated normalized stress intensity factor decreases with increasing the crack extension Δa. When Δa is very close to the crack tip stress concentration, the stress intensity factors become higher than the exact solution and the convergence of the solution will not be achieved. At crack extension of $0.01a$, the calculated stress intensity factor becomes within

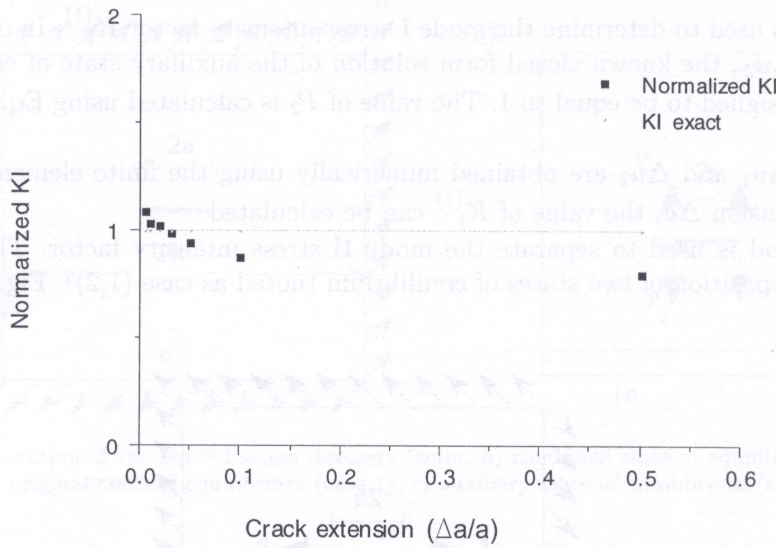

Fig. 9. The normalized stress intensity factor for mode I in a mixed mode problem versus the crack extension Δa

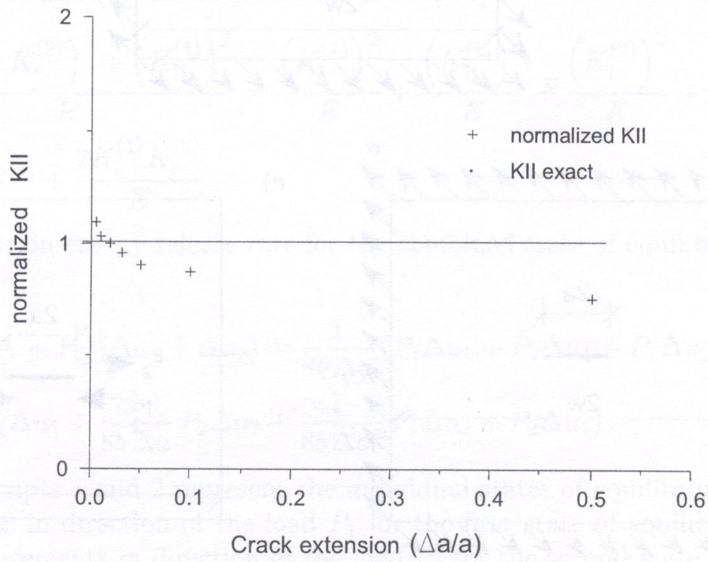

Fig. 10. The normalized stress intensity factor for mode II in a mixed mode problem versus the crack extension Δa

2% of the exact value. In the analyzed problem, the crack extension of $0.01a$ may be adopted to implement the technique.

4. Conclusion

A method of analysis based on the compliance technique and fundamental relationships is fracture mechanics has been proposed for determining the stress intensity factors K_{I} and K_{II} for pure mode I, pure mode II loading. The analysis is also suitable for separating the two stress intensity factors in a mixed mode problem. The present analysis can be conveniently conducted in conjunction with any numerical methods such as the finite element or boundary element methods. Good agreement between analytical exact solutions and present results has been demonstrated by solving problems available in the literature. Accuracy and convergence of the present method are not very sensitive to the finite element discretization of the continuum. It can be concluded form the analysis that selecting the crack extension Δa significantly influences the convergence of the solution. The crack extension Δa should be chosen away from the crack tip stress concentration and bounded by the limit where the closed form auxiliary solution applied. It appears that ratio $\Delta a/a$ should be selected within the range of 0.01 to 0.025″ in order for this method to converge to a good agreement with exact analysis within an acceptable accuracy.

Appendix

For the center-cracked sheet under pure mode I loading, the stress intensity factor is expressed as follows,

$$K_{\mathrm{I}} = \sigma\sqrt{\pi a}\left(\frac{1}{\cos\frac{\pi a}{2\omega}}\right)^{\frac{1}{2}} \tag{A1}$$

where a is half the crack length, and 2ω is the total width of the cracked sheet.

For pure mode II loading, a similar expression is used,

$$K_{\mathrm{II}} = \tau\sqrt{\pi a}\left(\frac{1}{\cos\frac{\pi a}{2\omega}}\right)^{\frac{1}{2}}. \tag{A2}$$

For the mixed mode loading, the separate values for K_{I} and K_{II} are

$$K_{\mathrm{I}} = \sigma\sqrt{\pi a}\,\sin^2\alpha \tag{A3}$$

$$K_{\mathrm{II}} = \sigma\sqrt{\pi a}\,\sin\alpha\,\cos\alpha \tag{A4}$$

For a crack in Fig. 7a the stress intensity factor K_{I} is

$$K_{\mathrm{I}} = \frac{P_2}{\sqrt{\pi a}}\sqrt{\frac{a+x_0}{a-x_0}} \tag{A5}$$

where x_0 is the distance between the force P_2 and the crack center.

References

[1] J.W. Eischen. Improve method for computing the J_2 Integral. *Engrg. Fract. Mech.*, **26**: 691, 1987.

[2] S.A. Hamoush, S.H. Ahmad. Mode I and mode II stress intensity factors for interfacial cracks in bi-material media. *Engrg. Fract. Mech.*, **33**(3): 421, 1989.

[3] S.A. Hamoush, M.R. Salami. Analyzing a mixed mode plane problem by using J_k integrals. *Int. J. Fatigue*, **12**(5): 441, 1990.

[4] S.A. Hamoush, M.R. Salami. Stiffness derivative technique to determine mixed mode stress intensity factors for rectilinear anisotropic solids. *Engrg. Fract. Mech.*, **44**(2): 297, 1993.

[5] A.G. Hermann, G. Hermann. On energy release for a plane crack. *ASME J Appl. Mech.*, **48**: 52, 1981.
[6] H.R. Irwin. Analysis of stress and strains near the end of a crack transversing a plate. *ASME J. Appl. Mech.*, **24**: 361, 1957.
[7] H. Tada, P.C. Paris, G.R. Irwin. *The Stress Analysis of Cracks Handbook.* Del Research, 1977.